



The study of the magnetic and room-temperature magnetocaloric properties in spin-reorientation $\text{Nd}_{1-x}\text{Dy}_x\text{Co}_4\text{Al}$ ($x = 0, 0.1$) alloys

S.C. Ma^a, D.H. Wang^{a,*}, C.L. Zhang^a, H.C. Xuan^a, S.D. Li^b, Z.G. Huang^b, Y.W. Du^a

^a National Laboratory of Solid State Microstructures and Key Laboratory of Nanomaterials for Jiang Su Province, Nanjing University, Hankou Road 22, Nanjing 210093, People's Republic of China

^b Department of Physics, Fujian Normal University, Fuzhou 350007, People's Republic of China

ARTICLE INFO

Article history:

Received 23 November 2009

Received in revised form 14 January 2010

Accepted 21 January 2010

Available online 1 February 2010

Keywords:

Spin-reorientation

Magnetocaloric effect

Magnetocrystalline anisotropy

ABSTRACT

The spin-reorientation and magnetocaloric property in $\text{Nd}_{1-x}\text{Dy}_x\text{Co}_4\text{Al}$ ($x = 0, 0.1$) alloys are investigated. These alloys undergo two successive spin-reorientation transitions around room-temperature, which results in a positive and negative magnetic entropy change, respectively. With the increasing applied field (< 30 kOe), these spin-reorientation alloys show wide working temperature interval and relatively large values of refrigerant capacity. The spin-reorientation material would be a promising candidate for room-temperature magnetic refrigerant.

© 2010 Elsevier B.V. All rights reserved.

1. Introduction

Recently, more and more attention has been paid to magnetic refrigeration based on magnetocaloric effect (MCE) of materials, especially near room temperature, since it has higher energy efficiency and lower environmental pollution compared to conventional gas-compressed refrigeration [1–8]. Up to date, the investigation of MCE is mainly focused on the magnetic materials possessing the first-order phase transitions (FOT) or the second-order ones (SOT). It has been understood that the field-induced metamagnetic transition can generally give rise to the large magnetic entropy change (ΔS_M) in FOT materials, which is usually associated with the significant hysteresis loops [1–6]. On the other hand, the SOT materials with a paramagnetic–ferromagnetic phase transition near Curie temperature are extensively studied, exhibiting the prominent reversibility for the temperature/magnetic field cycling and relatively wider temperature range of refrigeration [7,8]. It is well known that the spin-reorientation (SR) transition manifests itself by a rotation of the easy magnetization direction and is often accompanied by an abrupt change of the magnetization [9–11]. Therefore, MCE resulted from materials possessing the SR transition could be expected [12–15]. Until now, the MCE in SR materials is mostly obtained at relatively low temperature [12–15]. As a result, the investigation of room-temperature MCE in SR materials is of importance.

NdCo_5 is a ferromagnetic intermetallic compound crystallizing in a hexagonal CaCu_5 -type structure with $P6/mmm$ space group [16–19]. In this compound, the magnetocrystalline anisotropy (MCA) of Co sublattice favors the c axis (first-order anisotropic constant $K_{1\text{Co}} > 0$), while the Nd sublattice tends to have a planar (a – b plane) MCA ($K_{1\text{Nd}} < 0$) because of a negative value for the second-order Stevens factor α_J [15]. With the increasing temperature, it undergoes two SR transition [9]. For temperature below the first SR transition temperature $T_{\text{SR1}} = 242$ K [9], the MCA of Nd sublattice is larger than that of Co sublattice, and consequently, the total magnetic moment M_s lies in the basal plane [9–11,15]. When temperature is above the second SR transition temperature $T_{\text{SR2}} = 283$ K [9], the axial MCA of Co sublattice is dominant and thus the c axis becomes the easy magnetization direction. In the temperature range $T_{\text{SR1}} < T < T_{\text{SR2}}$, due to the strong competition between these two MCAs, the conical arrangement of M_s between the basal plane and the c axis is produced [9]. Accordingly, the arrangement of M_s undergoes plane-cone and cone-axis SR transitions, which occur around T_{SR1} and T_{SR2} , respectively. Upon partial substitution of Al for Co or Dy for Nd, T_{SR1} and T_{SR2} of the doped compounds would increase, comparing to the parent phase of NdCo_5 [18]. In the present work, two room-temperature SR transitions are observed in $\text{Nd}_{1-x}\text{Dy}_x\text{Co}_4\text{Al}$ ($x = 0, 0.1$) alloys and the magnetic and magnetocaloric properties for these two alloys are investigated.

2. Experimental

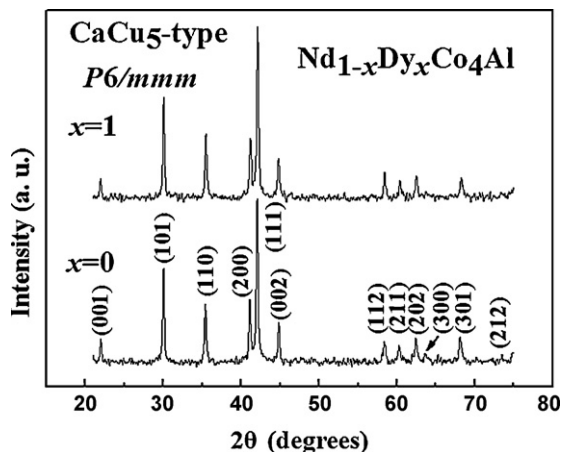
Polycrystalline specimens $\text{Nd}_{1-x}\text{Dy}_x\text{Co}_4\text{Al}$ ($x = 0, 0.1$) are synthesized by melting raw materials with stoichiometric proportion under a high-purity argon atmosphere, and then remelted up to three times to ensure homogeneity. The as-cast

* Corresponding author. Tel.: +86 25 83594588; fax: +86 25 83595535.

E-mail address: wangdh@nju.edu.cn (D.H. Wang).

Table 1The lattice parameters, SR transition temperatures and the maximum values of ΔS_M $\text{Nd}_{1-x}\text{Dy}_x\text{Co}_4\text{Al}$ ($x=0, 0.1$) alloys.

x	a (Å)	c (Å)	V (Å ³)	T_{SR1} (0.5 kOe) (K)	T_{SR2} (0.5 kOe) (K)	ΔS_M^{max} (J/kg K)	ΔS_M^{max} (J/kg K)
0	5.069	4.042	89.96	299	311	0.25 (10 kOe)	−0.88 (30 kOe)
0.1	5.055	4.043	89.48	305	317	0.15 (7 kOe)	−0.88 (30 kOe)

**Fig. 1.** XRD pattern for $\text{Nd}_{1-x}\text{Dy}_x\text{Co}_4\text{Al}$ ($x=0, 0.1$) alloys at room temperature.

ingots are sealed in evacuated quartz tubes and annealed at 1173 K for 7 days with a subsequent quench in cool-water. The hexagonal CaCu_5 -type structure ($P6/mmm$ space group) for both alloys is confirmed by X-ray powder diffraction (XRD) analysis at room temperature with $\text{Cu K}\alpha$ radiation. The lattice constants of these two alloys are listed in Table 1. Magnetic measurements are carried out using a superconducting quantum interference device magnetometer (Quantum Design) under a magnetic field up to 30 kOe.

3. Results and discussions

Fig. 1 reveals the XRD patterns for $\text{Nd}_{1-x}\text{Dy}_x\text{Co}_4\text{Al}$ ($x=0, 0.1$) alloys at room temperature. The diffraction peaks for NdCo_4Al alloy are indexed as the hexagonal CaCu_5 -type structure, which is consistent with the earlier reports [10,11,16–19]. For $\text{Nd}_{0.9}\text{Dy}_{0.1}\text{Co}_4\text{Al}$ alloy, it retains the same structure as the undoped one, but the diffraction peaks shift towards the high angle, suggesting the reduction of the cell volume due to the lanthanide contraction.

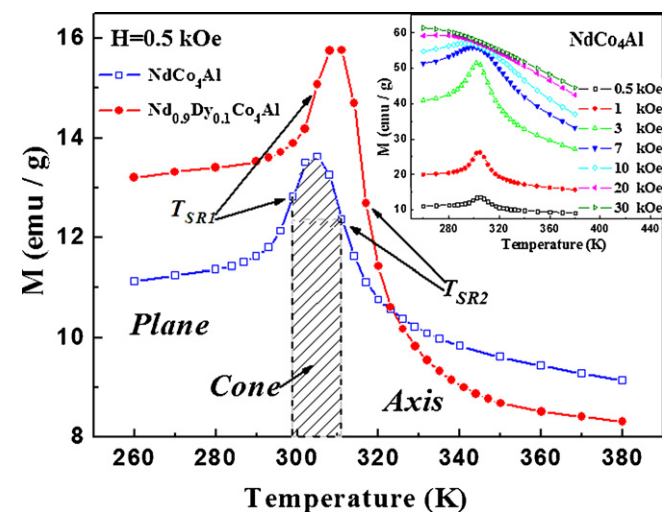
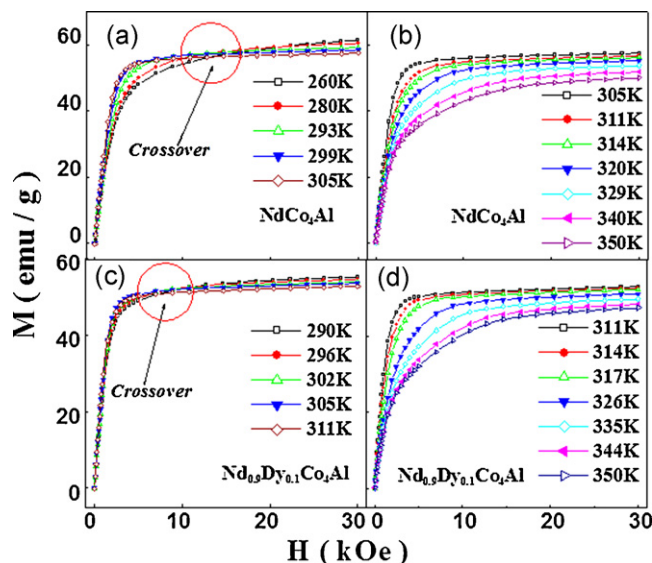
**Fig. 2.** Temperature dependence of the magnetization for $\text{Nd}_{1-x}\text{Dy}_x\text{Co}_4\text{Al}$ ($x=0, 0.1$) alloys under the field of 500 Oe. The inset presents the variation of the magnetization for NdCo_4Al alloy versus temperature at different applied field.

Fig. 2 presents the temperature dependence of the magnetization $M(T)$ curves under the field of 500 Oe for $\text{Nd}_{1-x}\text{Dy}_x\text{Co}_4\text{Al}$ ($x=0, 0.1$) alloys on heating. It can be seen that these alloys exhibit similar thermomagnetic behavior. First, the magnetization increases with the increase of temperature and peaks at a certain temperature. Further heating results in the decrease of the magnetization. Two SR transitions are observed during this temperature region. As we know, at low temperatures ($T < T_{\text{SR1}}$), the anisotropy of alloys are predominated by the R (Nd or Dy) contributions while the Co anisotropy prevails at higher temperatures ($T > T_{\text{SR2}}$). In the temperature range of $T_{\text{SR1}} < T < T_{\text{SR2}}$, the conical arrangement of M_s appears in these alloys as the R anisotropy is comparable with the Co anisotropy [20]. The temperature dependence of spin alignment in these alloys is denoted in Fig. 2 and the values of T_{SR1} and T_{SR2} of these alloys are listed in Table 1. With the Dy doping, both SR transition temperatures increase about 6 K due to the fact that the MCA energy of the Dy^{3+} is larger than that of Nd^{3+} [20]. It is worthy noting that all these transition temperatures are in the vicinity of room-temperature, which is important for application. Since the SR transition in this RCO_5 -type alloy is SOT [9,11], no thermal hysteresis is observed in $M(T)$ curves (not shown here). As shown in the inset of Fig. 2 (for clarity, we only present the result for NdCo_4Al here), the $M(T)$ curves show different behavior under different applied magnetic field. The first SR transition becomes more and more gentle with the increase of applied magnetic field and almost vanishes in the field of 30 kOe. This can be understood as a result of the competition between the Zeeman energy in the external field and the MCA energy [14].

A series of selected isothermal $M(H)$ curves for $\text{Nd}_{1-x}\text{Dy}_x\text{Co}_4\text{Al}$ ($x=0, 0.1$) alloys measured in heating run around T_{SR1} and T_{SR2} are plotted in Fig. 3. It is obvious that some crossovers are observed in the isotherms around T_{SR1} , as shown in Fig. 3(a) and (c). As we know, the absolute value of K_1 ($K_1 < 0$) of NdCo_4Al decreases with the increase of temperature around T_{SR1} , so the magnetization is easier to saturate at higher temperature [16]. On the other hand,

**Fig. 3.** Isothermal magnetization curves for $\text{Nd}_{1-x}\text{Dy}_x\text{Co}_4\text{Al}$: $x=0$ ((a) and (b)) and $x=0.1$ ((c) and (d)) around T_{SR1} and T_{SR2} , respectively.

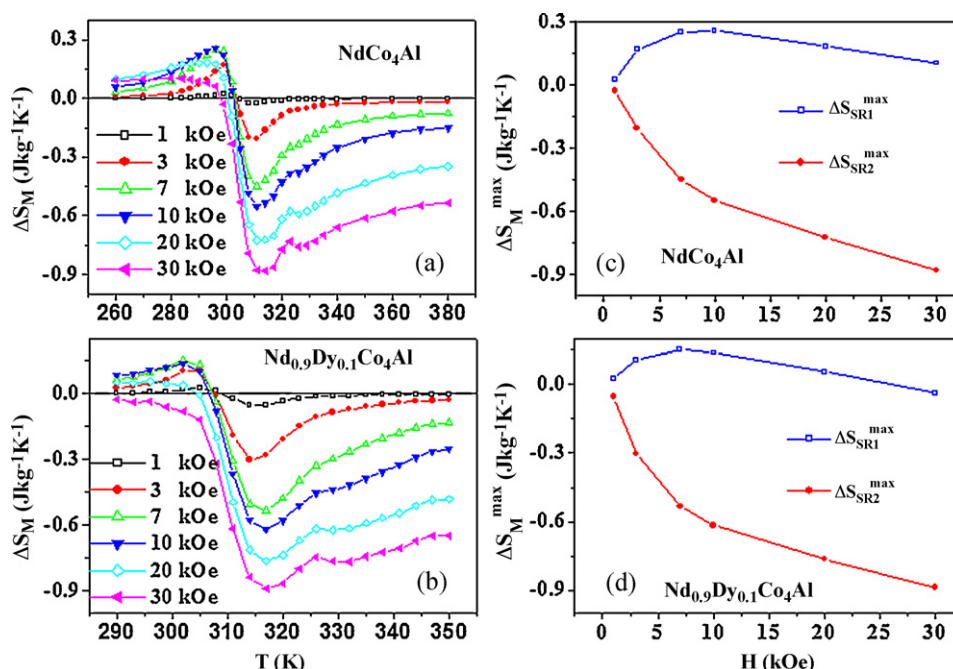


Fig. 4. Magnetic entropy change as a function of temperature for (a): NdCo₄Al and (b) Nd_{0.9}Dy_{0.1}Co₄Al alloys; (c) and (d) present the variation of the maximum magnetic entropy changes versus applied magnetic field around T_{SR1} and T_{SR2} for NdCo₄Al and Nd_{0.9}Dy_{0.1}Co₄Al alloys, respectively.

the magnetization of low temperature has a tendency to be larger than that of high temperature with the increasing external magnetic field, which can be seen from the inset of Fig. 2. These two reasons would be responsible for the crossovers in $M(H)$ curves around T_{SR1} . As for the $M(H)$ curves around T_{SR2} , the magnetization decreases monotonously with the increasing temperature. Note that the saturated magnetization decreases with the substitution for Dy element, which is ascribed to the ferrimagnetic coupling between the Dy and the Co moments in these compounds [11].

Based on the isothermal $M(H)$ curves and the Maxwell relation, the values of ΔS_M as a function of temperature in the field up to 30 kOe for Nd_{1-x}Dy_xCo₄Al ($x=0, 0.1$) around T_{SR1} and T_{SR2} are calculated and shown in Fig. 4(a) and (b). Some positive and negative ΔS_M peaks are observed around room-temperature, corresponding to the first and second SR transitions, respectively. It is obvious that the ΔS_M at T_{SR2} is larger than that at T_{SR1} , since the magnetization associated with the SR from cone to axis has a sharper change than that from plane to cone. The maximum value of ΔS_M at T_{SR2} is comparable with these of some ferromagnetic amorphous materials [21–23]. In addition, there are other kinks in the ΔS_M-T curves at 320 and 325 K, for $x=0$ and 0.1, respectively. At aforementioned temperatures, the second SR transition has completed and the second-order axial ferromagnetism to paramagnetism phase transition should start to occur. Since these two magnetic transitions have different ΔS_M at 320 or 325 K, some kinks would present in the $\Delta S_M(T)$ curves accordingly. Fig. 4(c) and (d) presents the applied magnetic field dependence of ΔS_M in these alloys. Interestingly, the peak values of positive ΔS_M do not increase monotonously with the increasing applied magnetic field and exhibit a maximum at a certain field (listed in Table 1), which can be understood by their thermomagnetic behavior in different external field shown in the inset of Fig. 2. In the case of the second SR, the values of ΔS_M increase and have a more and more gentle temperature dependence with the increasing magnetic field, which is consistent with their $M(T)$ curves. In addition, the maximum value of negative ΔS_M for Nd_{0.9}Dy_{0.1}Co₄Al is almost same as that of NdCo₄Al, but peaks at a higher temperature. The aforementioned two properties suggest a wide working temperature

range in these alloys, which is more beneficial for the application of magnetic refrigeration. On the other hand, the temperature region of positive ΔS_M is closer to that of negative ΔS_M for both alloys. The coexistence of two ΔS_M suggests that both the magnetizing and demagnetizing processes could be completed in one cooling cycle, which would enhance the efficiency and save energy of the magnetic refrigerator [24].

The peak values of ΔS_M are not the only parameter in characterizing the magnetocaloric properties. Another important aspect of evaluating a magnetic refrigerant is the refrigerant capacity (RC), which is connected to the entropy absorbed by the refrigerant at the cold end of the cycle and its temperature span. Here RC is obtained by integrating the area under the $\Delta S_M(T)$ curves, the integration limits using the temperature at half maximum of the ΔS_M peak [8,22]. The calculated values of RC at T_{SR2} are 34 and 37 J kg⁻¹ in the field of 20 kOe, for NdCo₄Al and Nd_{0.9}Dy_{0.1}Co₄Al, respectively, regardless of relatively small value of ΔS_M . Furthermore, the corresponding working temperature regions are 67 and 79 K, for NdCo₄Al and Nd_{0.9}Dy_{0.1}Co₄Al, respectively, which are larger than that of some second-order magnetic transition materials [25,26].

4. Conclusions

In conclusion, the SR transition is investigated in the Nd_{1-x}Dy_xCo₄Al ($x=0, 0.1$) alloys. With the Dy doping, SR transition temperatures increase about 6 K. The positive and negative ΔS_M peaks are observed in these alloys around T_{SR1} and T_{SR2} , respectively. These SR alloys have wide refrigerant temperature interval and relatively large RC. These results of Nd_{1-x}Dy_xCo₄Al ($x=0, 0.1$) alloys suggest that the SR material should be an alternative route for the search of room-temperature magnetic refrigerant.

Acknowledgement

This work is supported by the National Basic Research Program of China (2005CB623605), National Natural Science Foundation of

China (50701022 and 50831006) and the Program for New Century Excellent Talents of China (NCET-08-0278).

References

- [1] V.K. Pecharsky, K.A. Gschneidner Jr., Phys. Rev. Lett. 78 (1997) 4494–4497.
- [2] O. Tegus, E. Brück, K.H.J. Buschow, F.R. de Boer, Nature (London) 415 (2002) 150–152.
- [3] T. Krenke, E. Duman, M. Acet, E.F. Wassermann, X. Moya, L. Manosa, A. Planes, Nat. Mater. 4 (2005) 450–454.
- [4] F.X. Hu, B.G. Shen, J.R. Sun, Appl. Phys. Lett. 76 (2000) 3460–3462.
- [5] C.L. Zhang, D.H. Wang, Q.Q. Cao, Z.D. Han, H.C. Xuan, Y.W. Du, Appl. Phys. Lett. 93 (2008) 122505–122507.
- [6] Z.D. Han, D.H. Wang, C.L. Zhang, H.C. Xuan, B.X. Gu, Y.W. Du, Appl. Phys. Lett. 90 (2007) 042507–042509.
- [7] S. Yu. Dan'kov, A.M. Tishin, V.K. Pecharsky, K.A. Gschneidner Jr., Phys. Rev. B 57 (1998) 3478–3490.
- [8] Q.Y. Dong, B.G. Shen, J. Chen, J. Shen, H.W. Zhang, J.R. Sun, J. Appl. Phys. 105 (2009) 07A305.
- [9] J.B. Sousa, J.M. Moreira, A. Del Moral, P. Algarabel, R. Ibarra, J. Phys.: Condens. Matter 2 (1990) 3897–3902.
- [10] C. Zlotea, O. Isnard, J. Magn. Magn. Mater. 253 (2002) 118–129.
- [11] V. Klosek, C. Zlotea, O. Isnard, J. Phys.: Condens. Matter 15 (2003) 8327–8337.
- [12] O. Isnard, V. Pop, J.C. Toussaint, K.H.J. Buschow, J. Magn. Magn. Mater. 272–276 (2004) e335–e336.
- [13] M.I. Ilyn, A.V. Andreev, J. Phys.: Condens. Matter 20 (2008) 285206.
- [14] Q. Zhang, J.H. Cho, B. Li, W.J. Hu, Z.D. Zhang, Appl. Phys. Lett. 94 (2009) 182501–182503.
- [15] D.L. Rocco, J.S. Amaral, J.V. Leitão, V.S. Amaral, M.S. Reis, R.P. Fernandes, A.M. Pereira, J.P. Araújo, N.V. Martins, P.B. Tavares, A.A. Coelho, Phys. Rev. B 79 (2009) 014428.
- [16] K. Konno, H. Ido, S.F. Cheng, S.G. Sankar, W.E. Wallace, J. Appl. Phys. 73 (1993) 5929–5931.
- [17] H. Ido, W.E. Wallace, T. Suzuki, S.F. Cheng, V.K. Sinha, S.G. Sankar, J. Appl. Phys. 67 (1990) 4635–4637.
- [18] H. Ido, K. Konno, S.F. Cheng, W.E. Wallace, S.G. Sankar, J. Appl. Phys. 67 (1990) 4638–4640.
- [19] H. Ido, K. Konno, T. Ito, S.F. Cheng, S.G. Sankar, W.E. Wallace, J. Appl. Phys. 69 (1991) 5551–5553.
- [20] R.J. Radwański, J. Magn. Magn. Mater. 62 (1986) 120–126.
- [21] J.J. Ipus, J.S. Blázquez, V. Franco, A. Conde, L.F. Kiss, J. Appl. Phys. 105 (2009) 123922.
- [22] V. Franco, J.S. Blázquez, C.F. Conde, A. Conde, Appl. Phys. Lett. 88 (2006) 042505.
- [23] V. Franco, J.M. Borrego, A. Conde, S. Roth, Appl. Phys. Lett. 88 (2006) 132509.
- [24] X.X. Zhang, B. Zhang, S.Y. Yu, Z.H. Liu, W.J. Xu, G.D. Liu, J.L. Chen, Z.X. Cao, G.H. Wu, Phys. Rev. B 76 (2007) 132403.
- [25] Q. Zhang, X.G. Liu, F. Yang, W.J. Feng, X.G. Zhao, D.J. Kang, Z.D. Zhang, J. Phys. D: Appl. Phys. 42 (2009) 055011.
- [26] Q.Y. Dong, B.G. Shen, J. Chen, J. Shen, J.R. Sun, J. Appl. Phys. 105 (2009) 113902.